

Flood susceptibility mapping to improve models of species distributions

Elham Ebrahimi^{a,b,*}, Miguel B. Araújo^{c,d}, Babak Naimi^{d,e}

^a Swiss Federal Institute for Forest, Snow and Landscape Research WSL, Zürcherstrasse 111, 8903 Birmensdorf, Switzerland

^b Department of Biodiversity and Ecosystem Management, Environmental Sciences Research Institute, Shahid Beheshti University, Tehran, Iran

^c Department of Biogeography and Global Change, National Museum of Natural Sciences, CSIC, Madrid, Spain

^d Rui Nabeiro Biodiversity Chair, MED Institute, University of Évora, Évora, Portugal

^e Quantitative Biodiversity Dynamics (QBD), Department of Biology, University of Utrecht, Padualaan 8, Utrecht, 3584 CH, The Netherlands

ARTICLE INFO

Keywords:

Flood Susceptibility Indicator
Biodiversity Conservation
Species Distribution Models
Remote Sensing
Machine learning

ABSTRACT

As significant ecosystem disturbances flooding events are expected to increase in both frequency and severity due to climate change, underscoring the critical need to understand their impact on biodiversity. In this study, we employ advanced remote sensing and machine learning methodologies to investigate the effects of flooding on biodiversity, from individual species to broader ecological communities. Specifically, we utilized Sentinel-1 synthetic aperture radar (SAR) images and an ensemble of machine-learning algorithms to derive a flood susceptibility indicator. Our primary objective is to investigate the potential benefits of incorporating flood susceptibility, as a proxy for flood risk, into species distribution models (SDMs). By doing so, we aim to improve the performance of SDMs and gain deeper insights into the consequences of floods to biodiversity. Within the biodiverse landscape of the Zagros Mountains, a crucial Irano-Anatolian biodiversity hotspots, we examined the sensitivity of mammals, amphibians, and reptiles' distributions to flooding. Our analysis compared the performance of models that combined flood susceptibility with climate variables against models relying solely on climate variables. The results indicate that the inclusion of flood susceptibility significantly improves the capacity of models to explain and map species distributions for 67% of the species in our study region. Notably, amphibians and mammals are more profoundly affected by flooding compared to reptiles. The study highlights the importance of incorporating flood susceptibility as a predictor variable in species distribution models to improve the baseline characterization of potential species distributions. The importance of this variable will obviously depend on the regional context and the species studied but its relevance is likely to increase with climate change. In summary, our research demonstrates the integration of remote sensing and machine learning as a potent approach to advance biodiversity data science, monitoring, and conservation in the face of climate-induced flooding.

1. Introduction

Flooding is one of the most prominent disturbances and major natural disasters globally (Lugeri et al., 2010) that usually cause major damages to ecosystems and the environment (Zhang et al., 2021a). Floods can have significant impacts on biodiversity in many ways (Larsen et al., 2019; Maxwell et al., 2019) at various levels from individuals and species to communities and ecosystems (Kupika et al., 2021). Flooding can alter the structure and composition of ecosystems, reduce the availability of resources, increase the exposure to pathogens and pollutants, and cause mortality and displacement of species.

Compelling empirical evidence have already provided insights into the effects of flood events on species distribution and biodiversity for various groups, e.g., terrestrial animals (Golet et al., 2013; Zhang et al., 2021a), plants (Ferreira, 2000; Zhang et al., 2022) and African wildlife biodiversity (Kupika et al., 2021). Recent studies have demonstrated that the vulnerability of biodiversity to flood events varies among different species and over geographical locations (Bodmer et al., 2018; Connell et al., 2022; Horncastle et al., 2019; Pyhälä et al., 2016). Understanding the extent to which species are likely to be affected by floods is critical to inform natural area managements and biodiversity protection, particularly when species are already at risk of extinction. This

* Corresponding author at: Swiss Federal Institute for Forest, Snow, and Landscape Research WSL, ETH Zurich Domain, Zürcherstrasse 111, 8903 Birmensdorf, Switzerland.

E-mail address: Elham.ebrahimi@wsl.ch (E. Ebrahimi).

<https://doi.org/10.1016/j.ecolind.2023.111250>

Received 6 July 2023; Received in revised form 27 October 2023; Accepted 8 November 2023

Available online 16 November 2023

1470-160X/© 2023 The Author(s). Published by Elsevier Ltd. This is an open access article under the CC BY license (<http://creativecommons.org/licenses/by/4.0/>).

is specifically important because human-caused climate change is already resulting in an increased frequency and severity of extreme events, with dire consequences for biodiversity (Filazzola et al., 2021; Mahecha et al., 2020; Neilson et al., 2020) and floods are among such extreme events that account for a significant portion of natural disasters worldwide (Kron, 2015).

While flood is recognized as a potential significant driver affecting biodiversity and species distribution, its direct incorporation into ecological models (e.g., species distribution models; SDMs) presents a considerable challenge. The complexities lie in the dynamic and non-linear nature of flood events, the difficulty in determining threshold effects defining at what magnitude a flood event affects species, and species-specific responses to floods. Moreover, the interactions of floods with other environmental variables and the variability in data availability and quality further complicate the integration process. As a solution to these challenges, we suggest utilizing a flood susceptibility map offers a proxy and generalized indicator of flood risk. We argue that the incorporation of flood susceptibility as a variable in SDMs can overcome the challenges associated with modeling flood effects on biodiversity in a more standardized and data-driven manner. Therefore, to begin expanding our understanding of flood dynamics and its impacts on biodiversity, we propose mobilization of spaceborne satellite remote sensing technologies, along with machine learning approaches, can be an opportunity to evaluate the links between species occurrence and flood susceptibility that provide insights into understanding biodiversity patterns and changes.

Over the last two decades, the field of satellite technology has facilitated a quantum leap in our capacity to gather geospatial data. The emergence of Synthetic Aperture Radar (SAR) has revolutionized remote sensing capacity for flood mapping and monitoring (Li et al., 2018). This technology has the unique advantage of operating effectively under diverse weather conditions, allowing for reliable data collection and delineate water extent during flood events even under a dense cloud cover (Liang and Liu, 2020). Alongside, there has been a significant development in the European Space Agency's (ESA) Sentinel-1 mission which has made a wealth of public SAR images available for free, along with easy accessibility on cloud-based computational platforms such as Google Earth Engine (Clement et al., 2018; Munawar, 2022; Singha et al., 2020), setting a new milestone in flood assessments and risk mitigation (Benzougagh et al., 2022). Several studies already demonstrated the capacity of Sentinel-1 SAR images for accurately delineation of flood inundation areas (Cao et al., 2019; Liang and Liu, 2020), and flood susceptibility mapping (Shahabi et al., 2020), that makes them suitable for operational flood monitoring frameworks (Borah et al., 2018; Qiu et al., 2021).

Flood susceptibility mapping is a multi-step procedure that involves detection of flood areas, selecting relevant flood conditioning parameters, and constructing models using machine learning approaches. In recent years, many studies have applied various methods and techniques to improve the accuracy and efficiency of flood susceptibility mapping. For example, some studies have used different criteria and methods, such as frequency ratio, information value, entropy, and correlation analysis, to determine the most important parameters for flood susceptibility mapping (e.g., Wang et al., 2021). Other studies have employed and tested various machine learning models, such as neural networks, logistic regression, support vector machine, and random forest, to build and compare flood susceptibility models using various datasets and indicators (Liu et al., 2022). By taking the best out of these separate works, we came up with an integrated framework for flood susceptibility mapping using an ensemble of machine learning algorithms, trained by identified flood inundation areas based on SAR images. Such a framework can potentially enhance the performance and robustness of flood susceptibility mapping and provide useful information for flood risk management and mitigation.

This study aims to introduce a novel approach by incorporating a flood susceptibility map into SDMs to serve as a proxy for assessing flood

risk and to examine its potential to enhance the performance of SDMs. To the best of our knowledge, this research represents the first exploration of this innovative concept. The primary research question centers on understanding how individual species respond to varying degrees of flood risk and the resulting implications for species biodiversity, specifically species richness. Leveraging state-of-the-art Sentinel-1 SAR remote sensing technology and advanced machine learning methods, we investigate the impact of floods on species distributions in Zagros mountains, an ecologically significant mountainous region, and biodiversity hotspot in Iran that frequently experiences extreme meteorological events, including floods (Ahmadi et al., 2022; Razavi Termeh et al., 2018; Vaghefi et al., 2019; Yariyan et al., 2020). Our study places a special focus on a diverse group of terrestrial species, including mammals, amphibians, and reptiles, all of which may be particularly vulnerable to the effects of flooding (Bodmer et al., 2018; Jacob, 2003; Thibault and Brown, 2008). By shedding light on the relationships between floods and species distributions, this research offers insights into understanding the drivers of biodiversity dynamics that can inform the development of more effective conservation strategies and a deeper understanding of the risks faced by vulnerable species.

2. Material and method

2.1. Study area and description

Nested in the heart of the Irano-Anatolian biodiversity hotspot, the Zagros Mountains located in the southwestern Iran, span over 1500 km and represent one of the most important biodiversity hotspots in the Middle East. The region is a treasure trove of rich and diverse flora and fauna, providing a habitat for numerous endemic and critically threatened species (Ghane-ameleh et al., 2021; Karimi et al., 2023; Noroozi et al., 2018), comprising diverse habitats, including forests, shrublands, grasslands, and wetlands. The mountain range is characterized by dry summers and cold winters and receives most of its precipitation during the winter months. The study area in this research encompasses the Zagros Mountains, which have widely come under threat in recent years due to a combination of factors including the effects of climate change, extreme events, and poor conservation planning (Farashi and Shariati, 2017; Yousefi et al., 2020).

2.2. Flood susceptibility mapping

A general framework for modelling and mapping of flood susceptibility has been employed in many studies (e.g., Chapi et al., 2017) that links flood inventory data to topographic, climatic, and environmental conditions using a machine learning algorithm. In this study, we have advanced this approach by utilizing remotely sensed radar images to detect flood inundation areas. We trained an ensemble of multiple machine learning algorithms to map flood susceptibility and the methodology is summarized in Fig. 2.

2.2.1. Flood inundation areas

To identify inundation areas during flood events, we processed Sentinel-1 SAR images that were obtained between 2015 and 2022 (Fig. 1). To determine the dates of flood events or heavy rainfall that could cause flash floods in the region, we used half-hourly time series of precipitation grids, obtained from the integrated multi-satellite retrievals for the Global Precipitation Measurement (GPM) mission (IMERG; Huffman et al., 2020). For each identified flood event, we obtained Sentinel-1 Ground Range Detected (GRD) SAR bands (level-1; dual-polarization) for the period just before and after the event (hereafter, pre- and post-event).

To detect the flood inundation areas, we applied a pre-processing procedure to the images following Singha et al. (2020), which included a noise-removal. We then utilized a calibration threshold technique that compared backscatter intensity values in flooded and

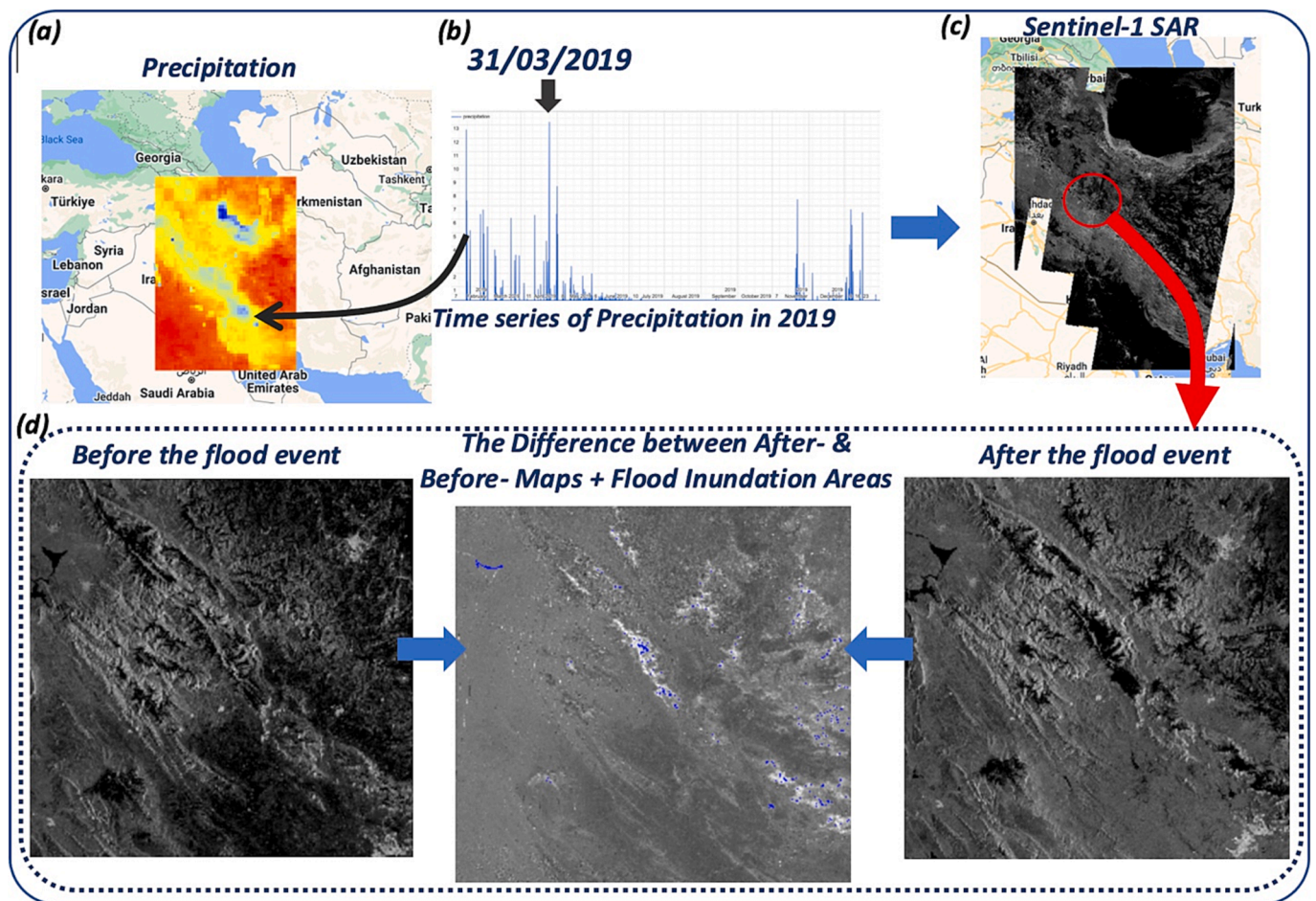


Fig. 1. Procedure for identifying flood inundation areas using Sentinel-1 SAR images; (a) map showing the mean precipitation based on half-hourly time series of precipitation grids obtained from Global Precipitation Management (GPM) mission; (b) example of a time series depicting precipitation values at a pixels with high mean precipitation, used to identify flood event dates for each year; (c) an example of Sentinel-1 SAR image over the study area; (d) Sentinel-1 SAR images obtained before- and after-flood event (for part of the study area), processed to identify flood inundation areas (the blue polygons in the middle image) by comparing the images before and after the flood event, representing as the “difference” image. (For interpretation of the references to colour in this figure legend, the reader is referred to the web version of this article.)

non-flooded areas. To differentiate pixels with permanent water bodies (e.g., lakes) from flooded areas, we used a modified normalized difference water index (NDWI) (Teng et al., 2021) derived from Sentinel-2 multi-spectral images at level 1-C (Du et al., 2016). This process allows us to establish a threshold below which water bodies and flooded areas could be identified. The post and pre-event images were then binarized using the threshold of -21 dB (Conde et al., 2019), and a binary map comparison method was employed to identify the flooded areas. All data acquisition and processing of this section were conducted in the Google Earth Engine platform. While this study primarily focused on assessing the influence of flood susceptibility on species distributions and biodiversity, we conducted a qualitative validation of the flood inundation areas identified through our SAR Sentinel-1 image processing. It is important to note that this validation was not aimed at quantitatively assessing spatial accuracy but rather at ensuring the reliability of the identified flood areas. To validate our results, we cross-referenced the detected flood events with official reports from the Iranian Meteorological Organization (IMO) and information obtained from trusted local news sources. By comparing the dates and locations of flood events reported by these authoritative sources with our dataset, we filtered out any discrepancies or inconsistencies. This approach allowed us to confirm that the identified flooded areas corresponded with documented flood events, enhancing the credibility of our dataset. A more detailed quantitative accuracy assessment of the inundation areas could

be a subject of future research to further strengthen the methodology.

We employed a spatial random sampling approach to draw a set of spatial data points within the identified flood areas, which were originally characterized as spatial polygons with areas ranging from 0.5 to 15 km^2 . These data points serve as representations of flood occurrences and were utilized as input data for the training of the machine learning algorithms, contributing to the development of flood susceptibility maps (see section 2.2.4).

2.2.2. Flood conditioning factors

After conducting an extensive literature review (Avand et al., 2022; Ghosh et al., 2022; Seydi et al., 2022; Yousefi et al., 2020b, Yousefi et al., 2020a; Zhao et al., 2018), we identified 9 flooding susceptibility features including digital elevation model (DEM), topographic slope, topographic wetness index (TWI), flow distance (vertical and horizontal), flow direction, flow accumulation, normalized difference vegetation index (NDVI), and precipitation (mean hourly precipitation over the last 20 years). To generate the topographic features, we used a DEM with 90 m spatial resolution, obtained from the shuttle radar topography mission (SRTM), which was pre-processed by filling the sink pixels to avoid any errors in hydrological analyses. The sink filling operation modifies an elevation value in a pixel that is smaller compared to its 8 neighboring pixels (Alkhouraji, 2020; Koriche, 2012). Using DEM as input, topographic slope, and flow direction layers were generated. The flow

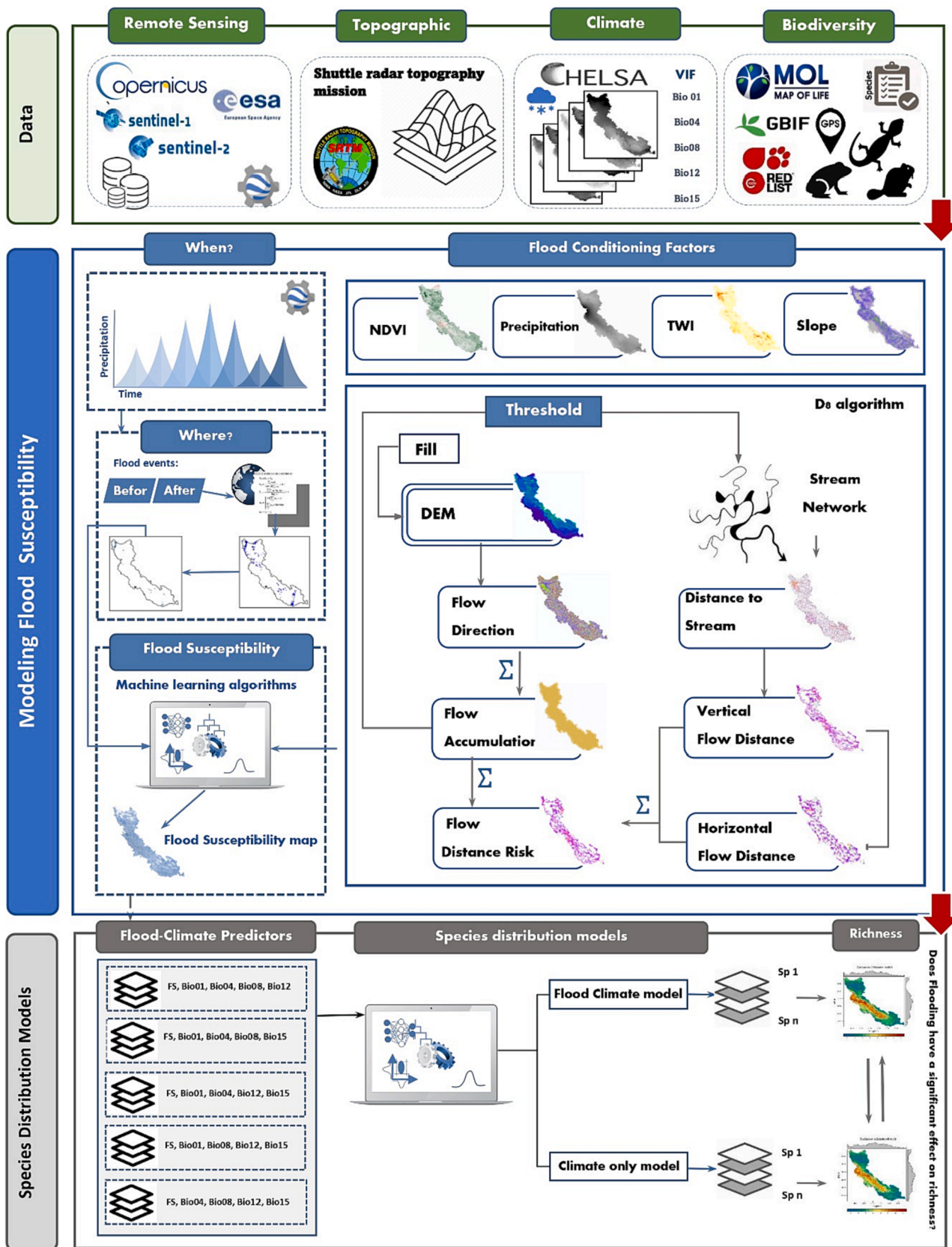


Fig. 2. Flowchart showing the methodology adopted in this study.

direction layer was generated using the D8 algorithm implemented in ESRI ArcGIS Pro (version 2.8), which determines the direction of flow at each pixel to its steepest downslope neighbor. The flow accumulation was then determined as the accumulated weight of all upstream pixels flowing into each downslope pixel. The magnitude of flows toward downstream also depends on the other conditions within the pixels (e.g., vegetation density), therefore, we calculated NDVI based on infrared and red bands of satellite images, obtained from Sentinel-2 (Notti et al., 2022), and averaged over eight annual cycles (2015–2022). We also considered the relative risk of flow distance as another flood conditioning factor. First, we extracted stream networks from the flow accumulation by applying a threshold such that the pixels with flow accumulation greater than the threshold (500) were classified as streams. We then calculated both the horizontal and vertical flow distances to the nearest stream using the stream network and the flow direction, and transformed these values, along with the flow accumulation value, into a single value of relative flow distance risk ranging between 0 and 1. The reasoning behind this is that a smaller distance to streams with greater flow accumulation increases the risk of flooding.

The next factor was TWI, which represents the influence of local topography on runoff flow direction and describes the tendency of a pixel to accumulate water (Gokceoglu et al., 2005; Mattivi et al., 2019). The equation (1) was used to calculate TWI (Beven and Kirkby, 1979; Moore et al., 1991):

$$TWI = \ln(\alpha/\tan\beta) \quad (1)$$

where α is the upstream catchment area, and $\tan \beta$ is the slope angle in degrees at each pixel.

2.2.3. Modeling flood susceptibility

We used six diverse machine learning algorithms for flood susceptibility modelling. These algorithms encompass a range of machine learning techniques and are grounded in different underlying assumptions, as is conventionally employed in flood susceptibility analysis (e.g., Mosavi et al., 2022; Shafizadeh-Moghadam et al., 2018; Youssef et al., 2022). They include Generalized Linear Models (GLM; Myers and Montgomery, 1997), Boosted Regression Trees (BRT; Elith et al., 2008), Random Forests (RF; Breiman, 2001), Support Vector Machine (SVM; Noble, 2006), Multivariate Adaptive Regression Spline (MARS; Friedman, 1991) and Maximum Entropy (MaxEnt; Phillips et al., 2006). This diversity allows us to account for a wide array of modeling techniques, effectively addressing the potential limitations and biases inherent in individual models. We then used an ensemble approach to combine the susceptibility maps generated by the individual models using a weighted averaging procedure. By employing the ensemble approach, we mitigate model-based uncertainty, which refers to the variability in predictions stemming from the choice of modeling techniques and parameterizations (Naghbi et al., 2017). This approach is consistent with the well-known documented benefits of ensemble forecasting, where the combination of models with varying assumptions and strengths yields more consistent and reliable predictions, ultimately minimizes errors or biases inherent in individual models (Araújo and New, 2007; Marmion et al., 2009).

We used flood inundation areas, generated through the processing of Sentinel-1 SAR images (section 2.2.1), to randomly draw a sample of 170 flood occurrence locations that were used as the response variable in the modeling process. We then generated a sample of 1000 random locations across the study area as background or pseudo-absence of flood event, which is necessary to train the machine learning models when the distribution of the response variable is binomial (Ghyoumi et al., 2022; Naimi and Araújo, 2016). Additionally, we used the 9 flood conditioning factors as predictor variables to train the machine learning algorithms. Before training the flood susceptibility models, we tested whether the predictor variables were subjected to multicollinearity problem by calculating their variance inflation factor (VIF) through a

stepwise procedure (Naimi et al., 2014). To evaluate the performance of the models, we used a bootstrapping procedure by randomly drawing a sample from the data (using sampling with replacement) and dividing the records into train and test partitions, which was repeated five times resulting in five replicates of train and test datasets. For each replicate, we fitted and evaluated the models using the training and test datasets, respectively. The area under the receiver operative characteristics curve (AUC) statistic was used to evaluate the performance of the models (Amiri et al., 2021; Fielding and Bell, 1997; Sheykhi Ilanloo et al., 2021). The AUC measures the ability of the models to correctly classify flood and non-flood locations, with a value of 1 indicating perfect discrimination and a value of 0.5 indicating random discrimination. A higher AUC value means that the model has a higher accuracy in predicting flood susceptibility (Harisena et al., 2021; Naimi and Araújo, 2016). Moreover, we calculated the importance of each variable using a permutation approach (Naimi and Araújo, 2016). We then used Jenks' natural break classification to divide the flood susceptibility map into five categories including Highest, High, Medium, Low, and Lowest. Jenks' method uses data segmentation to estimate the optimal break value to assign pixels to different classes. This method eliminates intraclass disparity and maximizes group disparity while increasing the average disparity within each class. A higher index rating represents areas that are particularly susceptible to flooding and vice versa (Chen et al., 2013).

2.3. Assessment of the effects of flood susceptibility on biodiversity

2.3.1. Target variable and predictor variable

Small species were given priority in our study due to their heightened susceptibility to the detrimental effects of floods, especially when compared to larger, less mobile species as highlighted in previous studies (Bodmer et al., 2018; Thibault and Brown, 2008). Our species occurrence data were meticulously sourced from a variety of reputable outlets, including research conducted by the first author, EE (Ebrahimi et al., 2021, 2022), as well as contributions from other researchers, and data from the global biodiversity information facility (GBIF). To ensure data accuracy and reliability, we subjected these records a stringent validation process. We cross-referenced them against the geographical range provided by the Map of Life (MOL) and the International Union for Conservation of Nature (IUCN). Further data quality control and cleaning procedure was carried out using the *CoordinateCleaner* package in R (Zizka et al., 2019), involving multiple criteria to identify and rectify common spatial and temporal errors in biodiversity data. These criteria included assessing general coordinate validity, detecting spatial and temporal outliers, resolving coordinate-country discrepancies, identifying, and removing duplicate coordinates per species, managing occurrences in seas and plains, addressing rounded and converted coordinates, and handling missing data. Following these steps, we performed spatial thinning, applying a distance threshold of 1 km based on the pixel size of the predictor variables (Naimi et al., 2022; Naimi and Araújo, 2016). These measures led to the exclusion of 193 records out of the initial 2252 records, leaving us with a robust dataset of 2058 reliable records representing 34 species, including 6 amphibians, 12 mammals, and 16 reptiles (see Table S.1 and Fig. S.1 for the checklist and corresponding distribution maps). To examine the impact of floods on species distributions, we integrated climate variables with flood susceptibility. Our climatic data was sourced from the CHELSA dataset (Karger et al., 2017), offering 19 bioclimatic variables spanning the period from 1979 to 2013, with a resolution of 30 arcseconds (approximately 1 km²). To address potential multicollinearity among the predictor variables, we employed a stepwise procedure, calculating variance inflation factors (VIF) for each variable at every step of the process. We then identified a variable with the highest VIF value, and if it was greater than the pre-defined threshold of 10, indicating collinearity, they were systematically excluded. This iterative procedure continued until all variables exhibited VIF values below the specified threshold (Naimi, 2022; Naimi et al.,

2014).

2.3.2. Species distribution models

To investigate the impact of floods on biodiversity, we constructed species distribution models using various subsets of climate and flood predictors. We employed eight different machine learning algorithms (see below) and a repeated bootstrapping resampling procedure that generated 100 replicates for each algorithm, resulting in a total of 800 models for each species. Each subset of predictors was restricted to 5 variables. We created two groups of models: one trained with climate-only predictors (referred to climate-only models), and another one trained with four climate variables and one flood susceptibility variable (referred to climate-flood models). Both groups contained 50 replicates for each modelling algorithm. We used five bioclimatic variables including Annual Mean Temperature (Bio1), Temperature Seasonality (Bio4), Mean Temperature of Wettest Quarter (Bio8), Annual Precipitation (Bio12), and Precipitation Seasonality (Bio15) (Karger et al., 2017). In the climate-flood group, the five subsets were created by replacing one of the bioclimatic variables with the flood susceptibility variable (for every 10 replicates out of 50 for each algorithm). We created 400 models for each group, and statistically compared the performance of the models between the two groups. We also assessed the contribution of the flood predictor to the models (Fig. 2).

The modelling algorithms include generalized linear models (GLM), generalized additive models (GAM), boosted regression trees (BRT), random forest (RF), support vector machine (SVM), multivariate adaptive regression spline (MARS), maximum entropy (MaxEnt), and DOMAIN. The 'sdm' R package (Naimi and Araújo, 2016) was used with default options to implement the models, and with an ensemble forecasting framework (Araújo and New, 2007) predictions were finally combined into a single consensus prediction. A bootstrapping method was employed for resampling of data and, dividing the records into train and test partitions, then the performance of each model was evaluated using the AUC (Ilanloo et al., 2020; Naimi et al., 2011) and true skill statistic (TSS) metrics (Allouche et al., 2006). Finally, a non-parametric statistical hypothesis test (Wilcoxon signed-rank test) was used to determine the significance of the flood susceptibility in improving the performance of SDMs in explaining the geographical distributions of species.

3. Results

3.1. Flood susceptibility models

We identified areas affected by the flood events by processing Sentinel-1 SAR images and the hourly time series of rainfall data between the years 2016 and 2022. A total of 170 flood points were drawn over the flood event polygons which have been used as the response variable in the flood susceptibility modelling.

All the nine flood conditioning factors were contributed to the flood susceptibility models as the results of the VIF test showed no sign of collinearity among the variables. The VIF values were less than 10 for all the variables (Table 1).

Based on the evaluation of the individual flood susceptibility models, measured using the AUC metric, it was found that Maxent and RF

exhibited the highest performance with AUC values of 0.9 and 0.89, respectively. Following closely, the models calibrated using BRT and MARS achieved AUC values of 0.86, followed by SVM and GLM with AUC of 0.83, and 0.8, respectively (Fig. 3).

The flood susceptibility map resulting from the ensemble approach, classified using Jenks' natural break classification, shows the zones with the highest flood susceptibility are mainly located to the north and south of the study area (Fig. 4). The ensemble approach predicts that 45.29 % of the study area falls within the lowest flood susceptibility zone, while 4.41 % falls within the highest flood susceptibility zone. The moderately flood-prone region covers 15.72 % of the study area, which is the highest percentage for this class among the models tested in this study.

The results of AUC-based permutation test to determine the relative importance of flood conditioning factors in explaining the flood susceptibility revealed that precipitation, DEM, and TWI were the most important variables, with the relative importance of 21.2 %, 16.3 %, and 23.1 %, respectively (Table 1).

3.2. Assessment of the effects of flood susceptibility on biodiversity

The Comparison between the models fitted in flood-climate and climate-only groups, in terms of their impact on biodiversity, showed that the models used flood susceptibility as a predictor performed significantly greater, based on TSS values, for 67 % of species (Fig. 5). Despite a high correlation coefficient (0.87) between the species richness maps generated by the two groups, the climate-flood models were more precise in mapping the areas with high richness values and limiting their extent compared to the climate-only models (Fig. 6). The variation of flood susceptibility values over pixels in areas with high and low species richness indicated a negative effect of floods on biodiversity (Fig. 7), which was confirmed by the Wilcoxon test (P -Value < 0.001). The inverse linear relationship between flood susceptibility and species richness was significant for all taxonomic groups (Fig. 8), with a weaker magnitude for reptiles (COR = -0.095) compared to amphibians (COR = -0.294) and mammals (COR = -0.208).

4. Discussion

Floods have long been recognized as a significant factor impacting biodiversity, however, their integration into ecological models presents a multifaceted challenge, remained a complex endeavor (Maxwell et al., 2019; Zhang et al., 2021b). Our study bridges this gap by introducing a novel approach that leverages flood susceptibility as a proxy for flood risk, offering fresh perspectives on the intricate relationship between floods and biodiversity. By utilizing remotely sensed Sentinel-1 SAR images and an ensemble of machine learning algorithms, we harnessed the power of flood susceptibility and its integration with climate variables within SDMs to explore the effects of flooding on the biodiversity of the Zagros Mountains in Iran not only at the species level but also at the community level, including species richness across taxonomic groups of mammals, amphibians, and reptiles. This novel concept underpins our research, marking the first instance where such an approach has been thoroughly tested. This evolution in our understanding of the relationship between floods and biodiversity opens new horizons for conservation efforts and ecological research in regions susceptible to

Table 1
Multicollinearity test among flood conditioning factors.

Factors	Collinearity Statistics	Variable importance	Factors	Collinearity Statistics	Variable importance
	VIF			VIF	
Slope	3.2	7.9 %	Flow direction	3.9	6.8 %
NDVI	2.8	9.9 %	Flow accumulation	2.1	8.3 %
TWI	4.6	11.8 %	DEM	8.5	17.5 %
Flow Distance Risk (v)	5.2	6.4 %	Precipitation	2.9	21.1 %
Flow Distance Risk (h)	6.3	10.3 %			

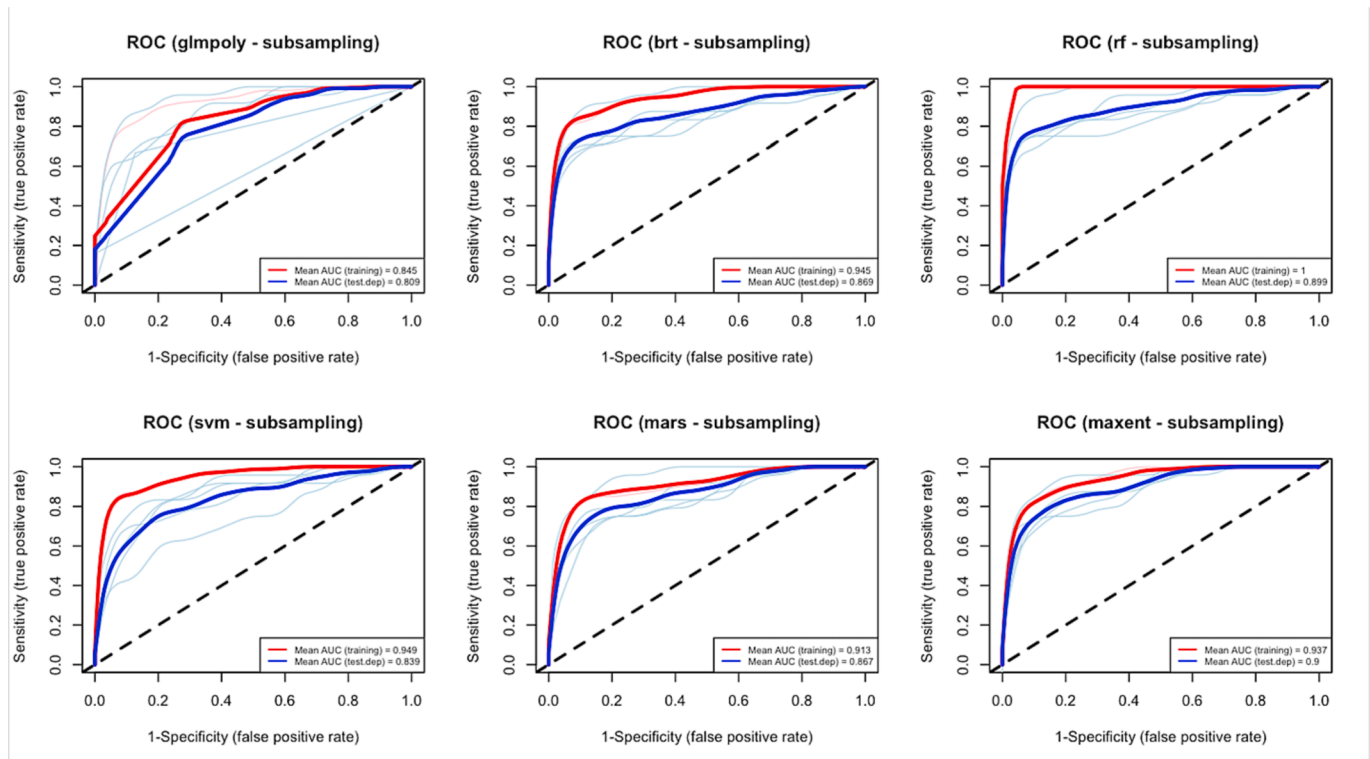


Fig. 3. ROC curve of the individual models.

extreme meteorological events.

The creative use of cutting-edge technologies has the potential to revolutionize biodiversity assessments and conservation efforts (Cavender-Bares et al., 2022; Martínez-López et al., 2015; Naimi and Voinov, 2012; Abbaspour et al., 2011). Several studies have emphasized the importance of critical technological advances for assessing extreme events such as fires (Kumar et al., 2022), droughts (Alahacoon and Edirisinghe, 2022), earthquakes (Xiang et al., 2022), avalanches (Singh et al., 2022), and hurricanes (Marlier et al., 2022). Our study demonstrates the integration of remote sensing radar imagery and advanced machine learning algorithms, combined with geospatial data analysis tools, to evaluate the effects of floods on biodiversity. This interdisciplinary approach showcases how technological advancements from various disciplines can enhance biodiversity assessments, contributing to more effective conservation strategies (Cavender-Bares et al., 2022). The study underscores the importance of interdisciplinary research in addressing complex ecological challenges.

Incorporating flood susceptibility as a predictor in SDMs resulted in more precise maps of species distributions and biodiversity richness in the Zagros Mountains, aligning with our expectations. However, an intriguing finding was a lower maximum richness value in flood-climate models compared to those using climate variables alone, indicating that floods can constrain species richness in the region. While climate variables are valuable for mapping potential species distributions, it is crucial to consider other abiotic and biotic factors that may limit species and biodiversity distributions (Peterson, 2011). The incorporation of these limiting factors into SDMs offers a more precise and realistic characterization of realized species distributions (Ilanloo et al., 2020). This insight highlights the complexity of ecological interactions and the importance of capturing them for effective conservation strategies.

In the intricate realm of multidimensional phenomena, such as flooding incidents, where numerous factors interact, ensemble machine learning models have demonstrated remarkable efficacy (Arabameri et al., 2019b, 2020). Ensemble techniques have significantly advanced flood susceptibility analysis, as supported by extensive research

(Arabameri et al., 2019a; Islam et al., 2023; Pham et al., 2021; Wang et al., 2021). These studies collectively underline the superior performance of ensemble models in unraveling the complexities of flood susceptibility. Our choice to adopt ensemble modeling is founded on the well-established principle that combining predictions from diverse models consistently yields more accurate results than relying solely on individual models (Araújo and New, 2007). This widely acknowledged principle in ecological modeling is substantiated by numerous studies (Le Lay et al., 2010; Marmion et al., 2009), confirming the superior predictive capacity of ensemble models. Furthermore, our comparative analysis validates the ensemble model's proficiency in delivering heightened precision and accuracy, consistent with previous research. Another notable advantage of the ensemble model lies in its ability to mitigate model-based uncertainty, resulting in more consistent and reliable predictions. This enhanced accuracy extends to spatial agreement, which assesses the model's ability to capture the spatial variability and heterogeneity of the phenomenon under investigation, a critical factor in flood susceptibility and species distribution analyses (Arabameri et al., 2020; Chapi et al., 2017).

We found that among the taxonomic groups considered, amphibians were most affected by flood susceptibility, followed by mammals, while reptiles showed a weak but significant inverse relationship with flood susceptibility (Fig. 8). The limited migration ability of amphibians makes them particularly vulnerable to floods, as noted by Adis and Junk (2002), and their distribution is considered as an indicator of habitat quality due to their rapid response to environmental changes (Beebe and Griffiths, 2005). Our findings support previous studies that suggest floods are a primary risk factor for amphibians (Lawler et al., 2010; Smith and Green, 2005). Additionally, our results suggest that floods can also affect small mammal distributions and population fluctuations (Anderson and Pezeshki, 2000; Jacob, 2003; Klinger, 2006; Thibault and Brown, 2008), consistent with Maxwell et al. (2019) and Zhang et al., (2021b), although some studies such as Wuczyński and Jakubiec (2013) have reported opposite findings. There is limited research on the effects of floods on reptiles, and our results showed a weak but significant

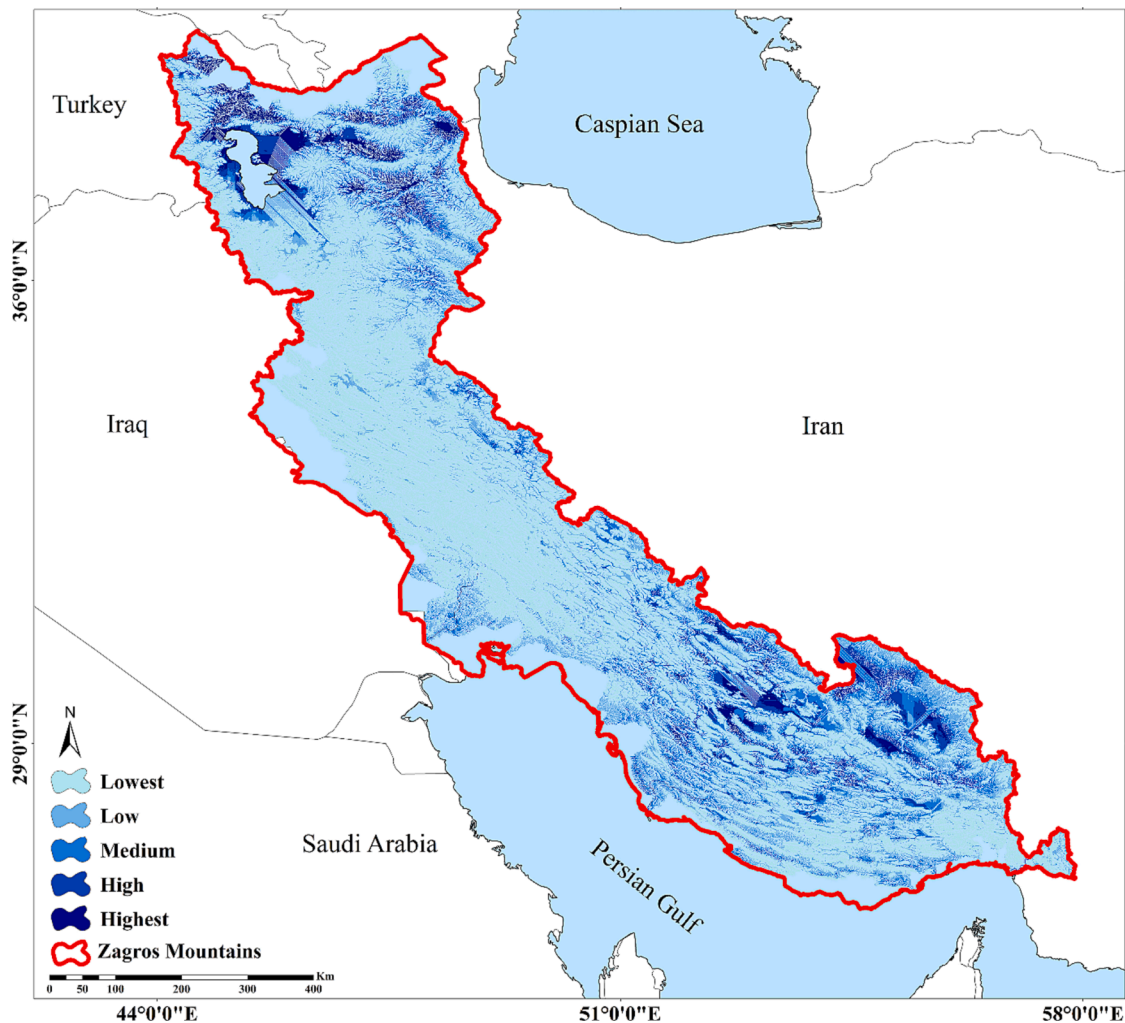


Fig. 4. Flood susceptibility maps derived from ensemble model.

inverse relationship between reptile richness and flood susceptibility, which may be related to their swimming ability and tolerance of aquatic conditions (Aubret et al., 2015; Richards and Clemente, 2013). More studies are needed to further understand the effects of floods on reptiles.

Despite floods being a significant limiting factor for most species, our results revealed that a small percentage (23 %) of species exhibited a positive response to floods. One possible explanation for this unexpected finding could be the biological traits of these species that make them less sensitive to floods (Thibault and Brown, 2008). Additionally, it is possible that these species have experienced historical disturbances that have enabled them to better cope with extreme events (Willmer et al., 2022). However, the presence of spatial sampling bias in the occurrence data cannot be ruled out as a contributing factor to this result. This issue is a well-known inherent problem with many species data and could potentially influence the accuracy of our model outputs (Cayuela et al., 2009; Keddy et al., 2009).

Our findings highlight the significance of precipitation as a key factor contributing to flood susceptibility (Table 1), which is consistent with previous studies (Rincón et al., 2018). Furthermore, previous research in the study area emphasized the pivotal role played by the combination of precipitation, land use, and geomorphology in determining flood potentials (Ahmadi et al., 2022). The interplay between these factors contributes to the overall vulnerability of the region, underscoring a need for comprehensive understanding and management strategies for mitigating the risks associated with flooding.

The approach and workflow developed in this study for analyzing the

effects of floods on biodiversity can be applied to other extreme events or potential drivers of biodiversity changes. Remote sensing data from various sources, including MODIS, Landsat, Aster, and Sentinel, have been extensively used to identify hazards, degradations, and extreme events (Kourosh Niya et al., 2019; Salati et al., 2014), as well as to delineate the boundaries of affected areas (Poursanidis and Chrysoulakis, 2017). If a variable of interest is a type of hazard or an extreme event, such as floods, landslides, or fires, the same machine learning approach used in this study for generating the susceptibility map can be employed when appropriate predictors that explain the event are selected. Alternatively, a remotely sensed product acting as proxies (Mokhtari et al., 2015) of some potential drivers, such as degradations, or erosions, could replace the susceptibility map in our workflow. These areas could be the subject of further investigation.

In this study, we have operated under the assumption that species distributions are primarily influenced by measurable biotic and abiotic factors at varying spatial resolutions. This foundational premise enables the application of our approach to any taxonomic group or geographic region with comparable data availability and quality. However, it is important to recognize that there may be additional unaccounted factors, including biotic interactions, dispersal limitations, evolutionary history, and human activities, that can influence species distributions. We encourage further research to encompass these factors in the analysis, aiming to assess the robustness and applicability of our approach across diverse spatial and temporal scales. Our approach offers practical implications for conservation planning and management.

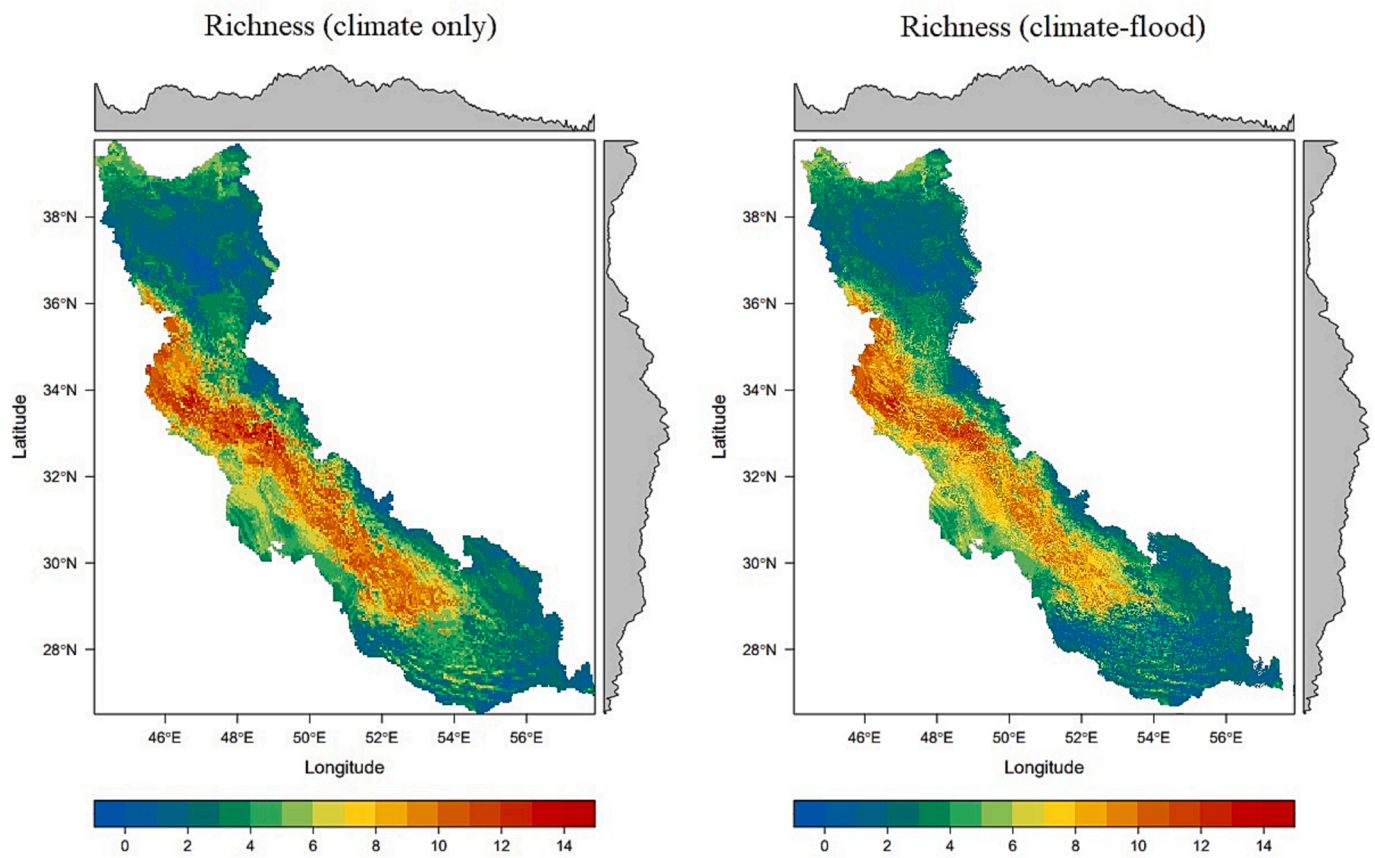


Fig. 6. Species richness generated by the climate-only and climatic-flood models; the gray graphs on the top and right of the map represent the richness variability over latitudes and longitudes, respectively.

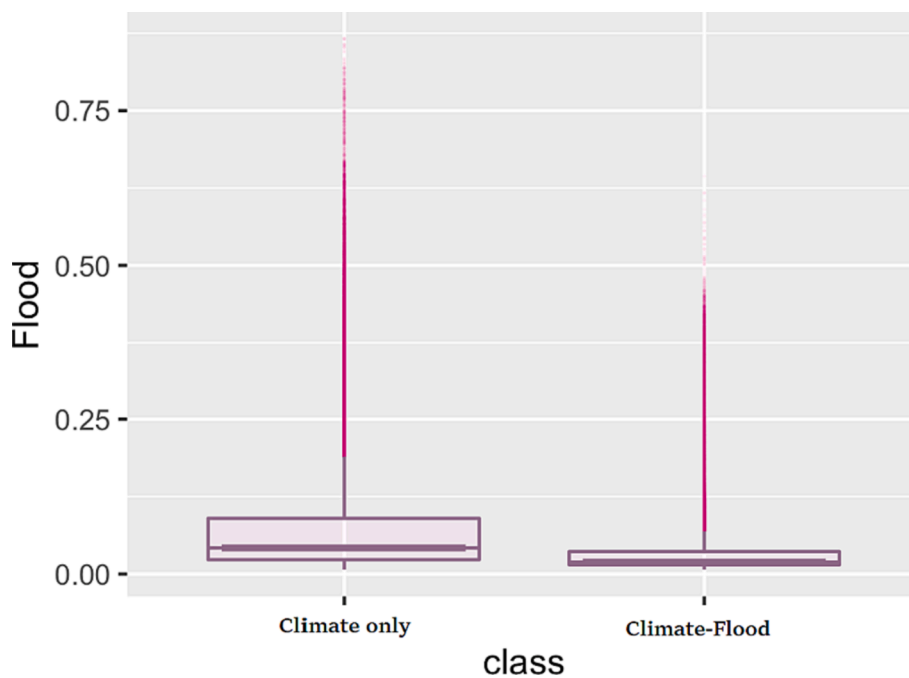


Fig. 7. Compare the relationship between flood susceptibility and species richness.

innovative approach provides fresh insights into the role of flood susceptibility as a critical predictor variable in species distribution models.

Our findings are consistent with evidence that floods have a critical

effect on the geographic distributions of species, affecting the overall diversity across regions and ecosystems. The integration of biodiversity data with remote sensing, machine learning, and geospatial data

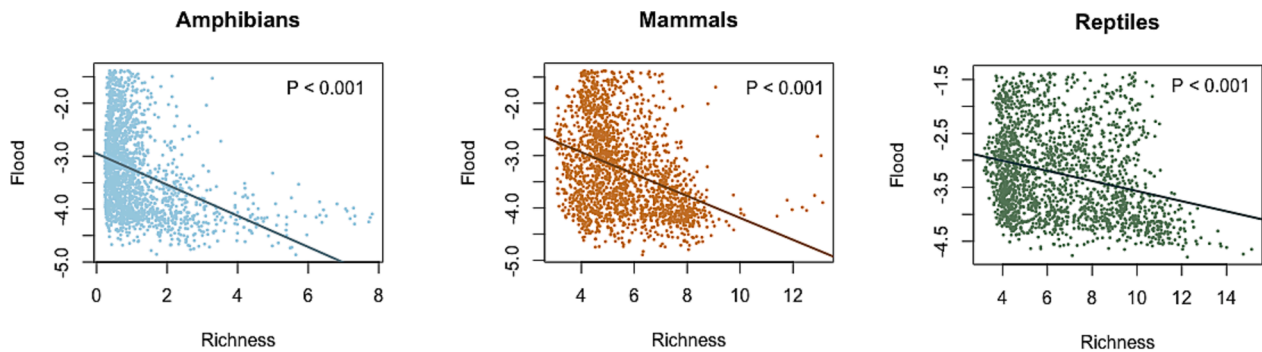


Fig. 8. Linear regressions between flood susceptibility and species richness of different taxonomic groups (amphibians, mammals, and reptiles); the P -values on the graph show that the negative relations between the species richness and flood are significant for all groups.

analysis opens promising avenues for advancing biodiversity science and unveiling intricate patterns that might otherwise remain hidden (Cavender-Bares et al., 2022). Specifically, our study highlights the critical role of flood susceptibility as a proxy for flood risk, and its importance in species distribution models to enhance the accuracy of mapping the realized distributions of species. By contributing to the growing body of literature on interdisciplinary approaches to biodiversity monitoring and conservation, our research emphasizes the urgent need for proactive measures and actions to combat ongoing biodiversity loss, driven by human activities and climate change. This study not only highlights the criticality of floods in shaping biodiversity but also offers a pioneering methodology for integrating flood risk into species distribution models, enhancing their effectiveness in mapping realized species distributions.

CRediT authorship contribution statement

Elham Ebrahimi: Conceptualization, Methodology, Visualization, Writing – original draft, Writing – review & editing. **Miguel B. Araújo:** Writing – review & editing. **Babak Naimi:** Supervision, Conceptualization, Methodology, Writing – review & editing.

Declaration of Competing Interest

The authors declare that they have no known competing financial interests or personal relationships that could have appeared to influence the work reported in this paper.

Data availability

Data will be made available on request.

Acknowledgements

We would like to express our gratitude to F. Ahmadzadeh and R. Sayahnia for generously providing the biodiversity fieldwork-based data in their lab. EE was supported by a research fellowship from ETH Zurich, Switzerland, and the National Elite Foundation of Iran.

Appendix A. Supplementary data

Supplementary data to this article can be found online at <https://doi.org/10.1016/j.ecolind.2023.111250>.

References

- Abbaspour, M., Mahiny, A.S., Arjmandy, R., Naimi, B., 2011. Integrated approach for land use suitability analysis 311–318.
- Adis, J., Junk, W.J., 2002. Terrestrial invertebrates inhabiting lowland river floodplains of Central Amazonia and Central Europe: a review. *Freshw. Biol.* 47, 711–731. <https://doi.org/10.1046/j.1365-2427.2002.00892.x>.

- Ahmadi, M., Derafshi, K., Mokhtari, D., Khodadadi, M., Najafi, E., 2022. Geodiversity assessments and geoconservation in the northwest of Zagros mountain range, Iran: grid and fuzzy method analysis. *Geoh Heritage* 14. <https://doi.org/10.1007/s12371-022-00769-7>.
- Alahacoon, N., Edirisinghe, M., 2022. A comprehensive assessment of remote sensing and traditional based drought monitoring indices at global and regional scale. *Geomatics. Nat. Hazards Risk* 13, 762–799. <https://doi.org/10.1080/19475705.2022.2044394>.
- Alkhouraji, W., 2020. GIS and DEM based watershed characteristics of Wadi Al-Adaira Basin. *KSA. Bull. La Société Géographique D'egypte* 93, 131–158. <https://doi.org/10.21608/bsge.2020.141584>.
- Allouche, O., Tsoar, A., Kadmon, R., 2006. Assessing the accuracy of species distribution models: prevalence, kappa and the true skill statistic (TSS). *J. Appl. Ecol.* 43, 1223–1232. <https://doi.org/10.1111/j.1365-2664.2006.01214.x>.
- Amiri, N., Vaissi, S., Aghamir, F., Saberi-Pirooz, R., Rödder, D., Ebrahimi, E., Ahmadzadeh, F., 2021. Tracking climate change in the spatial distribution pattern and the phylogeographic structure of Hyrcanian wood frog, *Rana pseudodalmatina* (Anura: Ranidae). *J. Zool. Syst. Evol. Res.* 59, 1604–1619. <https://doi.org/10.1111/jzs.12503>.
- Anderson, P.H., Pezeshki, S.R., 2000. The effects of intermittent flooding on seedlings of three forest species. *Photosynthetica*. <https://doi.org/10.1023/A:1007163206642>.
- Arabameri, A., Pradhan, B., Lombardo, L., 2019a. Comparative assessment using boosted regression trees, binary logistic regression, frequency ratio and numerical risk factor for gully erosion susceptibility modelling. *Catena* 183, 104223. <https://doi.org/10.1016/j.catena.2019.104223>.
- Arabameri, A., Rezaei, K., Cerdà, A., Conoscenti, C., Kalantari, Z., 2019b. A comparison of statistical methods and multi-criteria decision making to map flood hazard susceptibility in Northern Iran. *Sci. Total Environ.* 660, 443–458. <https://doi.org/10.1016/j.scitotenv.2019.01.021>.
- Arabameri, A., Saha, S., Mukherjee, K., Blaschke, T., Chen, W., Ngo, P.T.T., Band, S.S., 2020. Modeling spatial flood using novel ensemble artificial intelligence approaches in northern Iran. *Remote Sens.* 12, 1–30. <https://doi.org/10.3390/rs12203423>.
- Araújo, M.B., Anderson, R.P., Barbosa, A.M., Beale, C.M., Dormann, C.F., Early, R., Garcia, R.A., Guisan, A., Maiorano, L., Naimi, B., O'Hara, R.B., Zimmermann, N.E., Rahbek, C., 2019. Standards for distribution models in biodiversity assessments. *Sci. Adv.* 5, eaat4858. <https://doi.org/10.1126/sciadv.aat4858>.
- Araújo, M.B., New, M., 2007. Ensemble forecasting of species distributions. *Trends Ecol. Evol.* 22, 42–47. <https://doi.org/10.1016/j.tree.2006.09.010>.
- Aubret, F., Blanvillain, G., Kok, P.J.R., 2015. Myth busting? Effects of embryo positioning and egg turning on hatching success in the water snake *Natrix maura*. *Sci. Rep.* 5, 21–23. <https://doi.org/10.1038/srep13385>.
- Avand, M., Kuriqi, A., Khazaei, M., Ghorbanzadeh, O., 2022. DEM resolution effects on machine learning performance for flood probability mapping. *J. Hydro-Environment Res.* 40, 1–16. <https://doi.org/10.1016/j.jher.2021.10.002>.
- Beebee, T.J.C., Griffiths, R.A., 2005. The amphibian decline crisis: a watershed for conservation biology? *Biol. Conserv.* 125, 271–285. <https://doi.org/10.1016/j.biocon.2005.04.009>.
- Benzougagh, B., Frison, P.L., Meshram, S.G., Boudad, L., Dridri, A., Sadkaoui, D., Mimich, K., Khedher, K.M., 2022. Flood mapping using multi-temporal sentinel-1 SAR images: a case study—inaouene watershed from Northeast of Morocco. *Iran. J. Sci. Technol. - Trans. Civ. Eng.* 46, 1481–1490. <https://doi.org/10.1007/S40996-021-00683-Y/FIGURES/8>.
- Beven, K.J., Kirkby, M.J., 1979. A physically based, variable contributing area model of basin hydrology. *Hydro. Sci. Bull.* 24, 43–69. <https://doi.org/10.1080/02626667909491834>.
- Bodmer, R., Mayor, P., Antunez, M., Chota, K., Fang, T., Puertas, P., Pittet, M., Kirkland, M., Walkey, M., Rios, C., Perez-Peña, P., Henderson, P., Bodmer, W., Bicerria, A., Zegarra, J., Docherty, E., 2018. Major shifts in Amazon wildlife populations from recent intensification of floods and drought. *Conserv. Biol.* 32, 333–344. <https://doi.org/10.1111/COBI.12993>.
- Borah, S.B., Sivasankar, T., Ramya, M.N.S., Raju, P.L.N., 2018. Flood inundation mapping and monitoring in Kaziranga National Park, Assam using Sentinel-1 SAR data. *Environ. Monit. Assess.* 190. <https://doi.org/10.1007/s10661-018-6893-y>.
- Breiman, L., 2001. Random forests. *Mach. Learn.* 45, 5–32. <https://doi.org/10.1023/A:1010933404324>.

- Cao, H., Zhang, H., Wang, C., Zhang, B., 2019. Operational flood detection using Sentinel-1 SAR data over large areas. *Water (switzerland)* 11. <https://doi.org/10.3390/w11040786>.
- Cavender-Bares, J., Schneider, F.D., Santos, M.J., Armstrong, A., Carnaval, A., Dahlin, K. M., Fatoyinbo, L., Hurtt, G.C., Schimel, D., Townsend, P.A., Ustin, S.L., Wang, Z., Wilson, A.M., 2022. Integrating remote sensing with ecology and evolution to advance biodiversity conservation. *Nat. Ecol. Evol.* 6, 506–519. <https://doi.org/10.1038/s41559-022-01702-5>.
- Cayuela, L., Golicher, D.J., Newton, A.C., Kolb, M., de Albuquerque, F.S., Arets, E.J.M. M., Alkemade, J.R.M., Pérez, A.M., 2009. Species distribution modeling in the tropics: problems, potentialities, and the role of biological data for effective species conservation. *Trop. Conserv. Sci.* 2, 319–352. <https://doi.org/10.1177/194008290900200304>.
- Chapi, K., Singh, V.P., Shirzadi, A., Shahabi, H., Bui, D.T., Pham, B.T., Khosravi, K., 2017. A novel hybrid artificial intelligence approach for flood susceptibility assessment. *Environ. Model. Softw.* 95, 229–245. <https://doi.org/10.1016/j.envsoft.2017.06.012>.
- Chen, J., Yang, S., Li, H., Zhang, B., Lv, J., 2013. Research on geographical environment unit division based on the method of natural breaks (Jenks). *Int. Arch. Photogramm. Remote Sens. Spat. Inf. Sci. - ISPRS Arch.* 40, 47–50. <https://doi.org/10.5194/isprarchives-XL-4-W3-47-2013>.
- Clement, M.A., Kilsby, C.G., Moore, P., 2018. Multi-temporal synthetic aperture radar flood mapping using change detection. *J. Flood Risk Manag.* 11, 152–168. <https://doi.org/10.1111/jfr3.12303>.
- Conde, D., Solari, S., de Álava, D., Rodríguez-Gallego, L., Verrastro, N., Chreties, C., Lagos, X., Piñeiro, G., Teixeira, L., Seijo, L., Vitancurt, J., Caymaris, H., Panario, D., 2019. Ecological and social basis for the development of a sand barrier breaching model in Laguna de Rocha Uruguay. *Estuar. Coast. Shelf Sci.* 219, 300–316. <https://doi.org/10.1016/j.ecss.2019.02.003>.
- Connell, J., Hall, M.A., Nimmo, D.G., Watson, S.J., Clarke, M.F., 2022. Fire, drought and flooding rains: the effect of climatic extremes on bird species' responses to time since fire. *Divers. Distrib.* 28, 417–438. <https://doi.org/10.1111/ddi.13287>.
- Du, Y., Zhang, Y., Ling, F., Wang, Q., Li, W., Li, X., 2016. Water bodies' mapping from Sentinel-2 imagery with Modified Normalized Difference Water Index at 10-m spatial resolution produced by sharpening the swir band. *Remote Sens.* 8 <https://doi.org/10.3390/rs8040354>.
- Ebrahimi, E., Ranjbaran, Y., Sayahnia, R., Ahmadzadeh, F., 2022. Assessing the climate change effects on the distribution pattern of the Azerbaijan Mountain Newt (*Neurergus crocatus*). *Ecol. Complex.* 50, 100997 <https://doi.org/10.1016/j.ecocom.2022.100997>.
- Ebrahimi, E., Sayahnia, R., Ranjbaran, Y., Vaissi, S., Ahmadzadeh, F., 2021. Dynamics of threatened mammalian distribution in Iran's protected areas under climate change. *Mammalian Biol.* 101 (6), 759–774. <https://doi.org/10.1007/s42991-021-00136-z>.
- Elith, J., Leathwick, J.R., Hastie, T., 2008. A working guide to boosted regression trees. *J. Anim. Ecol.* 77, 802–813. <https://doi.org/10.1111/j.1365-2656.2008.01390.x>.
- Farashi, A., Shariati, M., 2017. Biodiversity hotspots and conservation gaps in Iran. *J. Nat. Conserv.* 39, 37–57. <https://doi.org/10.1016/j.jnc.2017.06.003>.
- Ferreira, L.V., 2000. Effects of flooding duration on species richness, floristic composition and forest structure in river margin habitat in Amazonian blackwater floodplain forests: Implications for future design of protected areas. *Biodivers. Conserv.* 9 <https://doi.org/10.1023/A:1008989811637>.
- Fielding, A.H., Bell, J.F., 1997. A review of methods for the assessment of prediction errors in conservation presence/absence models. *Environ. Conserv.* 24, 38–49.
- Filazzola, A., Matter, S.F., Macivor, J.S., 2021. Science of the total environment the direct and indirect effects of extreme climate events on insects. *Sci. Total Environ.* 769, 145161 <https://doi.org/10.1016/j.scitotenv.2021.145161>.
- Friedman, J.H., 1991. Multivariate adaptive regression splines. *Ann. Stat.* 19, 1–67. <https://doi.org/10.1214/aos/1176347963>.
- Ghane-ameleh, S., Khosravi, M., Saberi-pirooz, R., Ebrahimi, E., Asadi Aghbolaghi, M., Ahmadzadeh, F., 2021. Mid-Pleistocene transition as a trigger for diversification in the Irano-Anatolian region: evidence revealed by phylogeography and distribution pattern of the eastern three-lined lizard. *Glob. Ecol. Conserv.* 31, e01839 <https://doi.org/10.1016/j.gecco.2021.e01839>.
- Ghosh, S., Saha, S., Bera, B., 2022. Flood susceptibility zonation using advanced ensemble machine learning models within Himalayan foreland basin. *Nat. Hazards Res.* <https://doi.org/10.1016/J.NHRES.2022.06.003>.
- Ghyoumi, R., Ebrahimi, E., Mousavi, S.M., 2022. Dynamics of mangrove forest distribution changes in Iran. *J. Water Clim. Chang.* 13, 2479–2489. <https://doi.org/10.2166/wcc.2022.069>.
- Gokceoglu, C., Sonmez, H., Nefeslioglu, H.A., Duman, T.Y., Can, T., 2005. The 17 March 2005 Kuzulu landslide (Sivas, Turkey) and landslide-susceptibility map of its near vicinity. *Eng. Geol.* 81, 65–83. <https://doi.org/10.1016/j.enggeo.2005.07.011>.
- Golet, G.H., Hunt, J.W., Koenig, D., 2013. Decline and recovery of small mammals after flooding: implications for pest management and floodplain community dynamics. *River Res. Appl.* 29, 183–194. <https://doi.org/10.1002/RRA.1588>.
- Harisena, N.V., Groen, T.A., Toxopeus, A.G., Naimi, B., 2021. When is variable importance estimation in species distribution modelling affected by spatial correlation? *Ecography* 44 (5). <https://doi.org/10.1111/ecog.05534>.
- Horncastle, V.J., Chambers, C.L., Dickson, B.G., 2019. Grazing and wildfire effects on small mammals inhabiting montane meadows. *J. Wildl. Manage.* 83, 534–543. <https://doi.org/10.1002/jwmg.21635>.
- Huffman, G., Bolvin, D., Braithwaite, D., Hsu, K., Joyce, R., Kidd, C., N, E.J., Soroosh, S., S, E.F., Jackson, T., Wolff, D.B. and Pinging, X., 2020. Integrated Multi-satellite Retrievals for the Global Measurement (GPM) Mission (IMERG).
- Ilanloo, S.S., Ebrahimi, E., Valizadegan, N., Ashrafi, S., Rezaei, H.R., Yousefi, M., 2020. Little owl (*Athene noctua*) around human settlements and agricultural lands: conservation and management enlightenments. *Acta Ecol. Sin.* 40, 347–352. <https://doi.org/10.1016/j.chnaes.2020.06.001>.
- Islam, A.R.M.T., Bappi, M.M.R., Alqadhi, S., Bindajam, A.A., Mallick, J., Talukdar, S., 2023. Improvement of flood susceptibility mapping by introducing hybrid ensemble learning algorithms and high-resolution satellite imageries, *Natural Hazards*. Springer Netherlands. <https://doi.org/10.1007/s11069-023-06106-7>.
- Jacob, J., 2003. The response of small mammal populations to flooding. *Mamm. Biol.* 68, 102–111. <https://doi.org/10.1078/1616-5047-00068>.
- Karger, D.N., Conrad, O., Böhner, J., Kawohl, T., Kreft, H., Soria-Auza, R.W., Zimmermann, N.E., Linder, H.P., Kessler, M., 2017. Climatologies at high resolution for the earth's land surface areas. *Sci. Data* 4, 1–20. <https://doi.org/10.1038/sdata.2017.122>.
- Karimi, A., Yazdandad, H., Reside, A.E., 2023. Spatial conservation prioritization for locating protected area gaps in Iran. *Biol. Conserv.* 279, 109902 <https://doi.org/10.1016/j.biocon.2023.109902>.
- Keddy, P.A., Fraser, L.H., Solomeshch, A.I., Junk, W.J., Campbell, D.R., Arroyo, M.T.K., Alho, C.J.R., 2009. Wet and wonderful: the world's largest wetlands are conservation priorities. *Bioscience* 59, 39–51. <https://doi.org/10.1525/bio.2009.59.1.8>.
- Klinger, R., 2006. The interaction of disturbances and small mammal community dynamics in a lowland forest in Belize. *J. Anim. Ecol.* 75, 1227–1238. <https://doi.org/10.1111/j.1365-2656.2006.01158.x>.
- Koriche, S.A., 2012. Remote Sensing Based Hydrological Modelling for Flood Early Warning in the Upper and Middle Awash River Basin 67.
- Kourosh Niyaa, A., Huang, J., Kazemzadeh-Zow, A., Karimi, H., Keshkar, H., Naimi, B., 2019. Comparison of three hybrid models to simulate land use changes: a case study in Qeshm Island. *Iran. Environ. Monit. Assess.* 192 <https://doi.org/10.1007/s10661-020-08274-6>.
- Kron, W., 2015. Flood disasters - a global perspective. *Water Policy* 17, 6–24. <https://doi.org/10.2166/wp.2015.001>.
- Kumar, S., Getirana, A., Libonati, R., Hain, C., Mahanama, S., Andela, N., 2022. Changes in land use enhance the sensitivity of tropical ecosystems to fire-climate extremes. *Sci. Rep.* 12, 1–11. <https://doi.org/10.1038/s41598-022-05130-0>.
- Kupika, O.L., Gandiwa, E., Ayuk, J., Bandeira, S., Kunedzimwe, F., 2021. Evidence of the Impact of Cyclones and Floods on Biodiversity and Wildlife Resources in Southern Africa. https://doi.org/10.1007/978-3-030-74303-1_17.
- Larsen, S., Karaus, U., Claret, C., Sporka, F., Hamerlik, L., Tockner, K., 2019. Flooding and hydrologic connectivity modulate community assembly in a dynamic river-floodplain ecosystem. *PLoS One* 14, 1–22. <https://doi.org/10.1371/journal.pone.0213227>.
- Lawler, J.J., Shafer, S.L., Blaustein, A.R., 2010. Projected climate impacts for the amphibians of the western hemisphere. *Conserv. Biol.* 24, 38–50. <https://doi.org/10.1111/j.1523-1739.2009.01403.x>.
- Le Lay, G., Engler, R., Franc, E., Guisan, A., 2010. Prospective sampling based on model ensembles improves the detection of rare species. *Ecography (cop.)* 33, 1015–1027. <https://doi.org/10.1111/j.1600-0587.2010.06338.x>.
- Li, Y., Martinis, S., Plank, S., Ludwig, R., 2018. An automatic change detection approach for rapid flood mapping in Sentinel-1 SAR data. *Int. J. Appl. Earth Obs. Geoinf.* 73, 123–135. <https://doi.org/10.1016/j.jag.2018.05.023>.
- Liang, J., Liu, D., 2020. A local thresholding approach to flood water delineation using Sentinel-1 SAR imagery. *ISPRS J. Photogramm. Remote Sens.* 159 <https://doi.org/10.1016/j.isprsjprs.2019.10.017>.
- Liu, J., Wang, J., Xiong, J., Cheng, W., Li, Y., Cao, Y., He, Y., Duan, Y., He, W., Yang, G., 2022. Assessment of flood susceptibility mapping using support vector machine, logistic regression and their ensemble techniques in the Belt and Road region. *Geocart. Int.* 37 <https://doi.org/10.1080/10106049.2022.2025918>.
- Lugeri, N., Kundzewicz, Z.W., Genovesi, E., Hochrainer, S., Radziejewski, M., 2010. River flood risk and adaptation in Europe-assessment of the present status. *Mitig. Adapt. Strateg. Glob. Chang.* 15 <https://doi.org/10.1007/s11027-009-9211-8>.
- Mahecha, M.D., Gans, F., Brandt, G., Christiansen, R., Cornell, S.E., Fomferra, N., Kraemer, G., Peters, J., Bodesheim, P., Camps-Valls, G., Dinges, J.F., Dorigo, W., Estupinan-Suarez, L.M., Gutierrez-Velez, V.H., Gutwin, M., Jung, M., Londoño, M.C., Miralles, D.G., Papastefanou, P., Reichstein, M., 2020. Earth system data cubes unravel global multivariate dynamics. *Earth Syst. Dyn.* 11, 201–234. <https://doi.org/10.5194/esd-11-201-2020>.
- Marlier, M.E., Resetar, S.A., Lachman, B.E., Anania, K., Adams, K., 2022. Remote sensing for natural disaster recovery: lessons learned from Hurricanes Irma and Maria in Puerto Rico. *Environ. Sci. Policy* 132, 153–159. <https://doi.org/10.1016/j.envsci.2022.02.023>.
- Marmion, M., Parviainen, M., Luoto, M., Heikkinen, R.K., Thuiller, W., 2009. Evaluation of consensus methods in predictive species distribution modelling. *Divers. Distrib.* 15, 59–69. <https://doi.org/10.1111/j.1472-4642.2008.00491.x>.
- Martínez-López, J., Martínez-Fernández, J., Naimi, B., Carreno, M.F., Esteve, M.A., 2015. An open-source spatio-dynamic wetland model of plant community responses to hydrological pressures. *Ecol. Model.* 306, 326–333. <https://doi.org/10.1016/j.ecolmodel.2014.11.024>.
- Mattivi, P., Franci, F., Lambertini, A., Bitelli, G., 2019. TWI computation: a comparison of different open source GISs. *Open Geospatial Data, Softw. Stand.* 4 <https://doi.org/10.1186/s40965-019-0066-y>.
- Maxwell, S.L., Butt, N., Maron, M., McAlpine, C.A., Chapman, S., Ullmann, A., Segan, D. B., Watson, J.E.M., 2019. Conservation implications of ecological responses to extreme weather and climate events. *Divers. Distrib.* 25, 613–625. <https://doi.org/10.1111/ddi.12878>.
- Mohammadi, S., Ebrahimi, E., Shahriari Moghadam, M., Bosso, L., 2019. Modelling current and future potential distributions of two desert jerboas under climate change in Iran. *Ecol. Inform.* 52, 7–13. <https://doi.org/10.1016/j.ecoinf.2019.04.003>.

- Mokhtari, S., Hosseini, S.M., Danehkar, A., Azad, M.T., Kadlec, J., Jolma, A., Naimi, B., 2015. Inferring spatial distribution of oil spill risks from proxies: Case study in the north of the Persian Gulf. *Ocean Coast. Manag.* <https://doi.org/10.1016/j.ocecoaman.2015.08.017>.
- Moore, I.D., Grayson, R.B., Ladson, A.R., 1991. Digital terrain modelling: a review of hydrological, geomorphological, and biological applications. *Hydrol. Process.* 5, 3–30. <https://doi.org/10.1002/hyp.3360050103>.
- Mosavi, A., Golshan, M., Janizadeh, S., Choubin, B., Melesse, A.M., Dineva, A.A., 2022. Ensemble models of GLM, FDA, MARS, and RF for flood and erosion susceptibility mapping: a priority assessment of sub-basins. *Geocarto Int.* 37, 2541–2560. <https://doi.org/10.1080/10106049.2020.1829101>.
- Munawar, H.S., Hammad, A.W.A., Waller, S.T., 2022. Remote Sensing Methods for Flood Prediction: A Review. *Sensors* 2022, Vol. 22, Page 960 22, 960. <https://doi.org/10.3390/S22030960>.
- Myers, R.H., Montgomery, D.C., 1997. A tutorial on generalized linear models. *J. Qual. Technol.* 29, 274–291. <https://doi.org/10.1080/00224065.1997.11979769>.
- Naghibi, S.A., Moghaddam, D.D., Kalantar, B., Pradhan, B., Kisi, O., 2017. A comparative assessment of GIS-based data mining models and a novel ensemble model in groundwater well potential mapping. *J. Hydrol.* 548, 471–483. <https://doi.org/10.1016/j.jhydrol.2017.03.020>.
- Naimi, B., 2015. Babak Naimi. <https://doi.org/10.3990/1.9789036538404>.
- Naimi, B., Araújo, M.B., 2016. sdm: a reproducible and extensible R platform for species distribution modelling. *Ecography (cop.)* 39, 368–375. <https://doi.org/10.1111/ecog.01881>.
- Naimi, B., Capinha, C., Ribeiro, J., Rahbek, C., Strubbe, D., Reino, L., Araújo, M.B., 2022. Potential for invasion of traded birds under climate and land-cover change. *Glob. Chang. Biol.* 28, 5654–5666. <https://doi.org/10.1111/gcb.16310>.
- Naimi, B., Skidmore, A.K., Groen, T.A., Hamm, N.A.S., 2011. Spatial autocorrelation in predictors reduces the impact of positional uncertainty in occurrence data on species distribution modelling. *J. Biogeogr.* 38, 1497–1509.
- Naimi, B., Hamm, N.A.S., Groen, T.A., Skidmore, A.K., Toxopeus, A.G., 2014. Where is positional uncertainty a problem for species distribution modelling? *Ecography (cop.)* 37, 191–203. <https://doi.org/10.1111/j.1600-0587.2013.00205.x>.
- Naimi, B., Voinov, A., 2012. StellaR: A software to translate Stella models into R open-source environment. *Environ. Model. Softw.* 38, 117–118.
- Naimi, B., 2022. Package “usdm” Type Package Title Uncertainty Analysis for Species Distribution Models.
- Neilson, E.W., Lamb, C.T., Konkolics, S.M., Peers, M.J.L., Majchrzak, Y.N., Laura, D.D., April, G., Marting, R., Boutin, S., 2020. There’s a storm a-coming: Ecological resilience and resistance to extreme weather events 12147–12156. <https://doi.org/10.1002/ece3.6842>.
- Noble, W.S., 2006. What is a support vector machine? *Nat. Biotechnol.* 24, 1565–1567. <https://doi.org/10.1038/nbt1206-1565>.
- Noroozi, J., Talebi, A., Doostmohammadi, M., Rumpf, S.B., Linder, H.P., Schneeweiss, G. M., 2018. Hotspots within a global biodiversity hotspot-areas of endemism are associated with high mountain ranges. *Sci. Rep.* 8, 1–10. <https://doi.org/10.1038/s41598-018-28504-9>.
- Notti, D., Cignetti, M., Godone, D., Giordan, D., 2022. Semi-automatic mapping of shallow landslides using free Sentinel-2 and Google Earth Engine 1–34.
- Peterson, A.T., 2011. Ecological Niches and Geographic Distributions. <https://doi.org/10.1515/9781400840670>.
- Pham, B.T., Jaafari, A., Phong, T.V., Yen, H.P.H., Tuyen, T.T., Luong, V.V., Nguyen, H.D., Le, H.V., Foong, L.K., 2021. Improved flood susceptibility mapping using a best first decision tree integrated with ensemble learning techniques. *Geosci. Front.* 12, 101105. <https://doi.org/10.1016/j.gsf.2020.11.003>.
- Phillips, S.B., Aneja, V.P., Kang, D., Arya, S.P., 2006. Modelling and analysis of the atmospheric nitrogen deposition in North Carolina. *Int. J. Glob. Environ. Issues* 6, 231–252. <https://doi.org/10.1016/j.ecolmodel.2005.03.026>.
- Poursanisid, D., Chrysoulakis, N., 2017. Remote Sensing, natural hazards and the contribution of ESA Sentinels missions. *Remote Sens. Appl. Soc. Environ.* 6, 25–38. <https://doi.org/10.1016/j.rsase.2017.02.001>.
- Pyhälä, A., Fernández-Llamazares, A., Lehvävirta, H., Byg, A., Ruiz-Mallén, L., Salpeteur, M., Thornton, T.F., 2016. Global environmental change: Local perceptions, understandings, and explanations. *Ecol. Soc.* 21. <https://doi.org/10.5751/ES-08482-210325>.
- Qiu, J., Cao, B., Park, E., Yang, X., Zhang, W., Tarolli, P., 2021. Flood monitoring in rural areas of the pearl river basin (China) using sentinel-1 SAR. *Remote Sens.* 13. <https://doi.org/10.3390/rs13071384>.
- Razavi Termeh, S.V., Kornejady, A., Pourghasemi, H.R., Keesstra, S., 2018. Flood susceptibility mapping using novel ensembles of adaptive neuro fuzzy inference system and metaheuristic algorithms. *Sci. Total Environ.* 615, 438–451. <https://doi.org/10.1016/j.scitotenv.2017.09.262>.
- Reichstein, M., Camps-Valls, G., Stevens, B., Jung, M., Denzler, J., Carvalhais, N., 2019. Deep learning and process understanding for data-driven Earth system science. *Nature* 566, 195–204. <https://doi.org/10.1038/s41586-019-0912-1>.
- Richards, C.T., Clemente, C.J., 2013. Built for rowing: Frog muscle is tuned to limb morphology to power swimming. *J. r. Soc. Interface* 10. <https://doi.org/10.1098/rsif.2013.0236>.
- Rincón, D., Khan, U.T., Armenakis, C., 2018. Flood risk mapping using GIS and multi-criteria analysis: a greater toronto area case study. *Geo-Sciences.* <https://doi.org/10.3390/geosciences8080275>.
- Rocchini, D., Thouverai, E., Marcantonio, M., Iannacito, M., Da Re, D., Torresani, M., Bacaro, G., Bazzichetto, M., Bernardi, A., Foody, G.M., Furrer, R., Kleijn, D., Larsen, S., Lenoir, J., Malavasi, M., Marchetto, E., Messori, F., Montaghi, A., Moudrý, V., Naimi, B., Ricotta, C., Rossini, M., Santi, F., Santos, M.J., Schaeppman, M. E., Schneider, F.D., Schuh, L., Silvestri, S., Šimová, P., Skidmore, A.K., Tattoni, C., Tordoni, E., Vicario, S., Zannini, P., Wegmann, M., 2021. rasterdiv—an information theory tailored R package for measuring ecosystem heterogeneity from space: to the origin and back. *Methods Ecol. Evol.* 12. <https://doi.org/10.1111/2041-210X.13583>.
- Salati, S., van Ruitenbeek, F., van der Meer, F., Naimi, B., Salati, S., van Ruitenbeek, F., van der Meer, F., Naimi, B., 2014. Detection of alteration induced by onshore gas seeps from ASTER and worldview-2 data. *Remote Sens.* 6, 3188–3209. <https://doi.org/10.3390/rs6043188>.
- Seydi, S.T., Kanani-Sadat, Y., Hasanlou, M., Sahraei, R., Chanussot, J., Amani, M., 2022. Comparison of Machine Learning Algorithms for Flood Susceptibility Mapping. *Remote Sens.* 2023, Vol. 15, Page 192 15, 192. <https://doi.org/10.3390/RS15010192>.
- Shafizadeh-Moghadam, H., Valavi, R., Shahabi, H., Chapi, K., Shirzadi, A., 2018. Novel forecasting approaches using combination of machine learning and statistical models for flood susceptibility mapping. *J. Environ. Manage.* 217, 1–11. <https://doi.org/10.1016/j.jenvman.2018.03.089>.
- Shahabi, H., Shirzadi, A., Ghaderi, K., Omidvar, E., Al-Ansari, N., Clague, J.J., Geertsema, M., Khosravi, K., Amini, A., Bahrami, S., Rahmati, O., Habibi, K., Mohammadi, A., Nguyen, H., Melesse, A.M., Ahmad, B.B., Ahmad, A., 2020. Flood detection and susceptibility mapping using Sentinel-1 remote sensing data and a machine learning approach: hybrid intelligence of bagging ensemble based on K-Nearest Neighbor classifier. *Remote Sens.* 12. <https://doi.org/10.3390/rs12020266>.
- Sheykhi Ilanloo, S., Khani, A., Kafash, A., Valizadegan, N., Ashrafi, S., Loercher, F., Ebrahimi, E., Yousefi, M., 2021. Applying opportunistic observations to model current and future suitability of the Kopet Dagh Mountains for a Near Threatened avian scavenger. *Avian Biol. Res.* 14, 18–26. <https://doi.org/10.1177/1758155920962750>.
- Singh, K.K., Singh, D.K., Thakur, N.K., Dewali, S.K., Negi, H.S., Snehamani, M., V.d., 2022. Detection and mapping of snow avalanche debris from Western Himalaya, India using remote sensing satellite images. *Geocarto Int.* 37, 2561–2579. <https://doi.org/10.1080/10106049.2020.1762762>.
- Singha, M., Dong, J., Sarmah, S., You, N., Zhou, Y., Zhang, G., Doughty, R., Xiao, X., 2020. Identifying floods and flood-affected paddy rice fields in Bangladesh based on Sentinel-1 imagery and Google Earth Engine. *ISPRS J. Photogramm. Remote Sens.* 166, 278–293. <https://doi.org/10.1016/j.isprsjrs.2020.06.011>.
- Smith, M.A., Green, D.M., 2005. Dispersal and the metapopulation paradigm in amphibian ecology and conservation: Are all amphibian populations metapopulations? *Ecography (cop.)* 28, 110–128. <https://doi.org/10.1111/j.0906-7590.2005.04042.x>.
- Teng, J., Xia, S., Liu, Y., Yu, X., Duan, H., Xiao, H., Zhao, C., 2021. Assessing habitat suitability for wintering geese by using Normalized Difference Water Index (NDWI) in a large floodplain wetland China. *Ecol. Indic.* 122, 107260. <https://doi.org/10.1016/j.ecolind.2020.107260>.
- Thibault, K.M., Brown, J.H., 2008. Impact of an extreme climatic event on community assembly. *Proc. Natl. Acad. Sci. U. S. A.* 105, 3410–3415. <https://doi.org/10.1073/pnas.0712282105>.
- Vaghefi, S.A., Keykhai, M., Jahanbakhshi, F., Sheikholeslami, J., Ahmadi, A., Yang, H., Abbaspour, K.C., 2019. The future of extreme climate in Iran. *Sci. Rep.* 9, 1–11. <https://doi.org/10.1038/s41598-018-38071-8>.
- Wang, Y., Fang, Z., Hong, H., Costache, R., Tang, X., 2021. Flood susceptibility mapping by integrating frequency ratio and index of entropy with multilayer perceptron and classification and regression tree. *J. Environ. Manage.* 289. <https://doi.org/10.1016/j.jenvman.2021.112449>.
- Willmer, J.N.G., Püttker, T., Prevedello, J.A., 2022. Global impacts of edge effects on species richness. *Biol. Conserv.* 272, 109654. <https://doi.org/10.1016/j.biocon.2022.109654>.
- Wuczynski, A., Jakubiec, Z., 2013. Mortality of game mammals caused by an extreme flooding event in south-western Poland. *Nat. Hazards* 69, 85–97. <https://doi.org/10.1007/s11069-013-0687-x>.
- Xiang, M., Deng, Q., Duan, L., Yang, J., Wang, C., Liu, J., Liu, M., 2022. Dynamic monitoring and analysis of the earthquake Worst-hit area based on remote sensing. *Alexandria Eng. J.* 61, 8691–8702. <https://doi.org/10.1016/j.aej.2022.02.001>.
- Yariyan, P., Avand, M., Abbaspour, R.A., Torabi Haghighi, A., Costache, R., Ghorbanzadeh, O., Janizadeh, S., Blaschke, T., 2020. Flood susceptibility mapping using an improved analytic network process with statistical models. *Geomatics Nat. Hazards Risk* 11, 2282–2314. <https://doi.org/10.1080/19475705.2020.1836036>.
- Yousefi, S., Pourghasemi, H.R., Emami, S.N., Pouyan, S., Eskandari, S., Tiefenbacher, J. P., 2020a. A machine learning framework for multi-hazards modeling and mapping in a mountainous area. *Sci. Reports* 2020 101 10, 1–14. <https://doi.org/10.1038/s41598-020-69233-2>.
- Yousefi, S., Pourghasemi, H.R., Emami, S.N., Pouyan, S., Eskandari, S., Tiefenbacher, J. P., 2020b. A machine learning framework for multi-hazards modeling and mapping in a mountainous area. *Sci. Rep.* 10, 1–14. <https://doi.org/10.1038/s41598-020-69233-2>.
- Youssef, A.M., Pourghasemi, H.R., El-Haddad, B.A., 2022. Advanced machine learning algorithms for flood susceptibility modeling — performance comparison: Red Sea Egypt. *Environ. Sci. Pollut. Res.* 29, 66768–66792. <https://doi.org/10.1007/s11356-022-20213-1>.
- Zhang, X., Chan, N.W., Pan, B., Ge, X., Yang, H., 2021a. Mapping flood by the object-based method using backscattering coefficient and interference coherence of Sentinel-1 time series. *Sci. Total Environ.* 794, 148388. <https://doi.org/10.1016/j.scitotenv.2021.148388>.
- Zhang, Y., Li, Z., Ge, W., Chen, X., Xu, H., Guan, H., 2021b. Evaluation of the impact of extreme floods on the biodiversity of terrestrial animals. *Sci. Total Environ.* 790, 148227. <https://doi.org/10.1016/j.scitotenv.2021.148227>.

- Zhang, Y., Li, Z., Ge, W., Wang, J., Guo, X., Wang, T., Li, W., 2022. Assessment of the impact of floods on terrestrial plant biodiversity. *J. Clean. Prod.* 339 <https://doi.org/10.1016/j.jclepro.2022.130722>.
- Zhao, G., Pang, B., Xu, Z., Yue, J., Tu, T., 2018. Mapping flood susceptibility in mountainous areas on a national scale in China. *Sci. Total Environ.* 615, 1133–1142. <https://doi.org/10.1016/J.SCITOTENV.2017.10.037>.
- Zizka, A., Silvestro, D., Andermann, T., Azevedo, J., Duarte Ritter, C., Edler, D., Farooq, H., Herdean, A., Ariza, M., Scharn, R., Svantesson, S., Wengström, N., Zizka, V., Antonelli, A., 2019. CoordinateCleaner: Standardized cleaning of occurrence records from biological collection databases. *Methods Ecol. Evol.* 10, 744–751. <https://doi.org/10.1111/2041-210X.13152>.